UNIVERSITÀ DEGLI STUDI FIRENZE

FLORE
Repository istituzionale dell'Università degli Studi di Firenze

Lead isotope evidence for young trace element enrichment in the Oceanic Upper Mantle

Questa è la Versione finale referata (Post print/Accepted manuscript) della seguente pubblicazione:

Original Citation:

Lead isotope evidence for young trace element enrichment in the Oceanic Upper Mantle / A.N. HALLIDAY; G.R. DAVIES; D-C. LEE; S. TOMMASINI; C.R. PASLICK; J.G. FITTON; D.E. JAMES. - In: NATURE. - ISSN 0028-0836. - STAMPA. - 359:(1992), pp. 623-627. [10.1038/359623a0]

Availability:

This version is available at: 2158/224191 since:

Published version:

DOI: 10.1038/359623a0

Terms of use:

Open Access

La pubblicazione è resa disponibile sotto le norme e i termini della licenza di deposito, secondo quanto stabilito dalla Policy per l'accesso aperto dell'Università degli Studi di Firenze (https://www.sba.unifi.it/upload/policy-oa-2016-1.pdf)

Publisher copyright claim:

(Article begins on next page)

27 April 2024

nature

INTERNATIONAL WEEKLY JOURNAL OF SCIENCE

Volume 359 No. 6396 15 October 1992 £3.00

DIPARTIMENTO DI SCIENZE

AUTENTICAZIONE A TERGO

42>
9 770028 083019

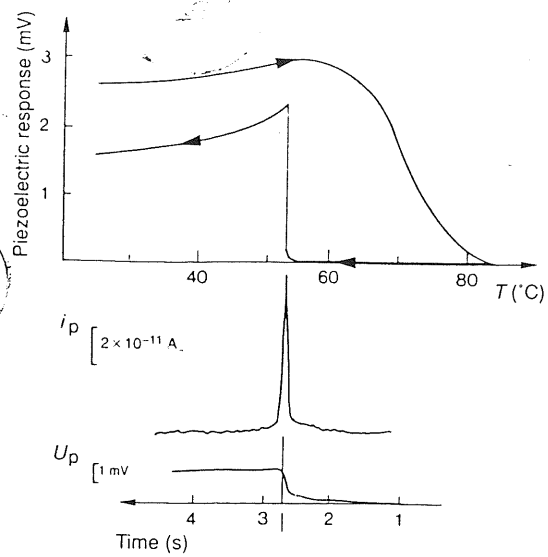

FIG. 4 The temperature behaviour of the piezoelectric response during heating the spontaneously polarized sample of M70 and subsequent cooling cycle. The spontaneous transition to the polar state occurs in the smectic X′ phase at $T = 53$ °C. The associated jump of the piezoresponse $U_p(t)$ and the corresponding pulse of the repolarization current $i(t)$ flowing through the electrometric amplifier ('fast feedback' mode) are shown below.

spontaneous polarization P_s at the transition is calculated to be in the range 1-1.5 nC cm^{-2} for the mixture M70 (for U_p signals of 2-3 mV). At room temperature, spontaneously repolarized samples show a stable piezoelectric response.

We have determined other properties characteristic of ferroelectric materials. First, optical second-harmonic generation[10] (1.06 μm) has been observed on unoriented samples of M70. Second, pyroelectric measurement[11] on I allowed us to calculate its macroscopic polarization (~4 nC cm^2).

We can thus conclude that the polyphilic compounds investigated show ferroelectric properties. The smectic X′ phase consists of polar domains which can spontaneously realign. The direction of the macroscopic polarization can be switched, both in the X and X′ phases, by an external field, with hysteresis loops typical of ferroelectrics. No electro-optical effect has been observed during the spontaneous transition; this means that macroscopic polarizations of opposite signs correspond to the same refractive index ellipsoid, as should be the case for longitudinal ferroelectrics. But no firm conclusion can yet be drawn about the mechanism involved in the ferroelectric behaviour of these new materials. The combination of the polyphilic character with longitudinal and transverse molecular dipole moments could produce a variety of ferroelectric and antiferroelectric packings. Boundary effects and layer curvatures might also contribute to the behaviour. □

Received 29 January; accepted 5 August 1992.

1. Goodby, J. W. *et al.* (eds) *Ferroelectric Liquid Crystals* (Gordon and Breach, Philadelphia, 1991).
2. Meyer, R. B., Liébert, L., Strzelecki, L. & Keller, P. *J. Phys.* (Paris) **36**, L69-L71 (1975).
3. Tournilhac, F., Bosio, L., Nicoud, J. F. & Simon, J. *Chem. Phys. Lett.* **145**, 452-454 (1988).
4. Tournilhac, F. & Simon, J. *Ferroelectrics* **114**, 283-287 (1991).
5. Beresnev, L. A., Blinov, L. M., Osipov, M. A. & Pikin, S. A. *Molec. Cryst. Liq. Cryst.* **A158**, 1-150 (1988).
6. Walba, D. M. *et al. J. Am. chem. Soc.* **113**, 5471 (1991).
7. Prost, J. & Barois, P. *J. chim. Phys.* **80**, 65-80 (1983).
8. Petschek, R. G. & Wiefling, K. M. *Phys. Rev. Lett.* **59**, 343-346 (1987).
9. Blinov, L. M., Davidyan, S. A., Petrov, A. G., Todorov, A. T. & Yablonsky, S. V. *JETP Lett.* (in Russian) **48**, 259-262 (1988).
10. Kurtz, S. K. & Perry, T. T. *J. appl. Phys.* **39**, 3798-3813 (1968).
11. Blinov, L. M. *et al. Liq. Cryst.* **2**, 121-130 (1987).

ACKNOWLEDGEMENTS. We thank L. A. Beresnev for supplying conventional ferroelectrics, L. Bosio for X-ray measurements, D. Subachuys for pyroelectric measurements, V. Lemoine for his contribution to nonlinear optical experiments and J. Prost for discussions.

Lead isotope evidence for young trace element enrichment in the oceanic upper mantle

Alex N. Halliday*, Gareth R. Davies*, Der-Chuen Lee*, Simone Tommasini*, Cassi R. Paslick*, J. Godfrey Fitton† & Dodie E. James†

* Department of Geological Sciences, University of Michigan, Ann Arbor, Michigan 48109-1063, USA
† Department of Geology and Geophysics, University of Edinburgh, Edinburgh EH9 3JW, UK

ISOTOPIC heterogeneity in ocean island basalts has generally been ascribed to processes related to the long-term cycling of mantle material[1-6]. A recent study of Cameroon line lavas reported higher $^{208}Pb/^{204}Pb$ and $^{206}Pb/^{204}Pb$ ratios towards the continent/ocean boundary (c.o.b.), but no corresponding increase in $^{207}Pb/^{204}Pb$, indicating large *in situ* fractionations of uranium and thorium relative to lead in the upper mantle ~10^8 years ago[7]. Here we present neodymium, strontium and lead isotope data for a variety of central Atlantic islands, and show that similar offsets in lead isotope ratios are found in lavas from the islands of Madeira and Trinidade. Like the Cameroon line c.o.b. lavas, these lavas are characterized by high U/Pb and Ce/Pb, low K/U and are located in areas of old oceanic lithosphere[8]. But in contrast to the Cameroon line[7], the Madeira lavas are derived from an enriched MORB-type source with low $^{207}Pb/^{204}Pb$ and $^{87}Sr/^{86}Sr$ and high $^{143}Nd/^{144}Nd$. The lead isotope data can be explained if the U/Pb ratios in the sources are comparable to those observed for the lavas and the U/Pb fractionation occurred at the time of formation of the local oceanic lithosphere. Although we do not have a satisfactory explanation for the U/Pb fractionation, it must have occurred at shallow depths in the mantle, near a spreading ridge; and the resulting enriched source regions have since remained fixed relative to the migrating lithosphere.

Isotopic compositions of continental intraplate mantle-derived magmas commonly vary as a function of lithospheric age[9,10]. Oceanic lithosphere, however, is young and effectively of uniform age relative to continental lithosphere. As a consequence any isotopic effects generated by *in situ* decay are

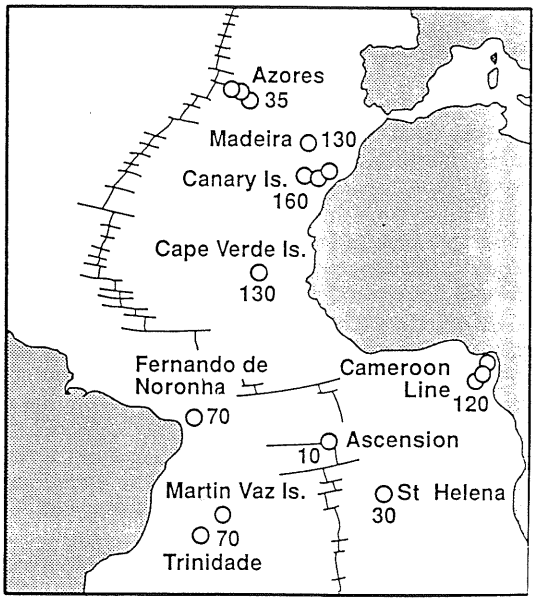

FIG. 1 Map of the central Atlantic Ocean showing locations of OIB volcanic centres. Numbers indicate the age (in Myr) of the local lithosphere[8].

TABLE 1 isotope data for Central Atlantic OIBs

Sample number	Rock type	MgO (wt%)	$^{87}Rb/^{86}Sr$	$^{147}Sm/^{144}Nd$	$^{238}U/^{204}Pb$	$^{87}Sr/^{86}Sr$	$^{143}Nd/^{144}Nd$	$^{206}Pb/^{204}Pb$	$^{207}Pb/^{204}Pb$	$^{208}Pb/^{204}Pb$
Madeira										
MD4	alkali basalt	6.5	0.0868	0.1178	40.8	0.702895±13	0.513045±9	19.060	15.440	38.578
MD10	basanite	7.5	0.0780	0.1196	44.8	0.702888±11	0.513063±9	19.208	15.545	38.867
MD32	basanite	12.8	0.0839	0.1233	43.5	0.703032±11	0.513053±8	19.047	15.491	38.683
MD40	alkali basalt	10.7	0.0814	0.1311	35.1	0.702782±11	0.513109±9	19.049	15.490	38.567
MD64	basanite	8.1	0.0838	0.1193	43.0	0.702802±13	0.513113±7	18.949	15.458	38.447
Ascension										
AS1	transitional basalt	5.1	0.1606	0.1344	37.4	0.702847±9	0.513000±8	19.473	15.672	39.190
AS3	transitional basalt	5.3	0.1194	0.1398	22.4	0.702792±9	0.513033±6	19.259	15.619	38.864
AS5	transitional basalt	4.2	0.1737	0.1365	29.4	0.702753±13	0.513058±6	19.431	15.646	39.081
AS10	transitional basalt	4.6	0.1165	0.1323	22.4	0.702913±13	0.513003±5	19.658	15.660	39.311
Trinidade										
TD3	olivine nephelinite	13.4	0.1635	0.1186	26.7	0.703611±11	0.512762±8	19.047	15.564	38.816
TD4	nephelinite	5.6	0.0691	0.0791	52.0	0.703804±13	0.512772±8	19.143	15.535	39.023
TD5	nephelinite	6.6	0.0261	0.1440	44.5	0.703837±9	0.512799±9	19.152	15.523	39.020
Azores-Fayal										
AZFY1	alkali basalt	6.6	0.0732	0.1261	23.2	0.703931±11	0.512863±6	19.153	15.634	38.937
AZFY2	alkali basalt	10.2	0.1329	0.1333	21.1	0.703762±14	0.512930±9	19.058	15.595	38.717
AZFY3	alkali basalt	8.6	0.2059	0.1254	9.62	0.703886±11	0.512878±8	18.637	15.606	38.350
Azores-Pico										
AZP5	transitional basalt	16.2	0.0227	0.1387	20.0	0.703696±14	0.512911±7	19.432	15.610	38.938
AZP6	alkali basalt	6.2	0.1064	0.1249	28.9	0.703443±13	0.512946±6	19.464	15.604	38.936
AZP7	alkali basalt	16.1	0.1146	0.1372	16.6	0.703748±14	0.512885±6	18.755	15.552	38.251
AZP8	alkali basalt	13.2	0.1238	0.1299	19.6	0.703943±14	0.512869±6	19.295	15.676	39.082
Azores-Flores										
AZF1	alkali basalt	4.8	0.1738	0.1107	29.3	0.703380±12	0.512969±7	19.282	15.582	38.990
AZF2	alkali basalt	6.1	0.1806	0.1092	25.8	0.703360±13	0.512934±8	19.289	15.565	38.836
AZF3	transitional basalt	10.6	0.0697	0.1213	26.9	0.703364±8	0.512945±8	19.002	15.546	38.626

All isotopic ratios measured at the University of Michigan using a VG Sector multicollector mass spectrometer. $^{147}Sm/^{144}Nd$ and $^{238}U/^{204}Pb$ measured by isotope dilution at the University of Michigan. MgO and $^{87}Rb/^{86}Sr$ determined by X-ray fluorescence at the University of Edinburgh. Uncertainties in isotopic ratios refer to least significant digits and represent $\pm 2\sigma$ mean run precisions. Sr and Nd isotopic compositions are presented normalized to $^{86}Sr/^{88}Sr=0.1194$ and $^{146}Nd/^{144}Nd=0.7219$, respectively, and were measured in multidynamic mode. Pb isotopic ratios are presented normalized to NBS SRM981 using a fractionation correction of 0.101% per a.m.u. and were measured in static mode. The $^{87}Sr/^{86}Sr$ of NBS SRM987 was 0.71025 ± 1 (2σ, N=20) and the $^{143}Nd/^{144}Nd$ of the La Jolla Nd standard was 0.51185 ± 1 (2σ, N=20) at the time of these analyses.

likely to be small compared with those inherited from asthenospheric heterogeneities. The central Atlantic is an ideal location in which to study the relationships between the lithosphere and isotopic compositions in basalts because the range in lithospheric age is large[8], there are no recent subduction zones nearby and the area is well away from the effects of the Dupal anomaly in the Southern Hemisphere[5,11]. The locations of the main intraplate volcanic centres in the central Atlantic region are shown in Fig. 1. The age of the adjacent oceanic lithosphere ranges from close to zero (Ascension) to ~160 Myr (Canary Islands)[8].

New Nd, Sr and Pb isotope data, together with parent/daughter ratios for basaltic lavas, from several of these islands are presented in Table 1, and plotted in Fig. 2, along with previous data for a variety of other ocean island basalts (OIBs) and mid-ocean-ridge basalts (MORBs)[12,19]. Details of the geology of the islands studied here can be found elsewhere (refs 8, 13–15, 20–24 and refs therein). The least well known are Trinidade and Madeira. Trinidade is a volcanic cone rising 5,500 m above sea level and is dominated by rocks undersaturated in silica, in the form of pyroclastic deposits, domes, dykes and plugs, together with subordinate lava flows that include nephelinite, ankaratrite and phonolite, all of which are dated at <4 Myr (ref. 21). Madeira is the main island of an archipelago, and the rocks are dominated by alkaline olivine basalts and their differentiates (chiefly hawaiites and mugearites) that are unusually rich in Na, and have been dated at >3 Myr (refs 22, 23).

The Nd and Sr isotopic compositions for Madeira, the Cameroon line and Trinidade, situated in areas of old lithosphere, are not significantly different from those for islands closer to the Mid-Atlantic Ridge such as the Azores, Ascension and St Helena (Fig. 2*a*). For example, both Ascension and Madeira are characterized by very radiogenic Nd and unradiogenic Sr plotting within the MORB field, and the Cameroon line c.o.b. samples show similarities to HIMU or Lo-Nd islands such as St Helena. But although Madeira, Trinidade and the Cameroon line c.o.b. show correlated variations in $^{208}Pb/^{204}Pb$ and $^{206}Pb/^{204}Pb$ and plot within the general MORB–OIB array (Fig. 2*b*), there is no correlation with $^{207}Pb/^{204}Pb$. Instead, these volcanic centres define fields that are displaced to the right of the array for other OIB and MORB in Fig. 2*c*. This is evidence of both extreme and young source enrichments in U and Th relative to Pb (ref. 7). The shorter half-life of ^{235}U results in it having a much lower abundance at present relative to ^{238}U. Because U and Th are believed to have similar distribution coefficients during mantle melting, a large fractionation in U/Pb is associated with change of similar magnitude in Th/Pb. The time-integrated effect of these fractionations in the recent past (say 100 Myr ago) will be correlated changes in $^{206}Pb/^{204}Pb$ and $^{208}Pb/^{204}Pb$, at relatively constant $^{207}Pb/^{204}Pb$. Because U and Th are more incompatible than Pb during mantle melting[6,7,16,25–27], limits can be placed on the time needed to generate the offsets shown in Fig. 2*c*, given an upper limit for the source U/Pb ratio corresponding to the measured values for the lavas (Table 1). The lavas of these three regions are characterized by unusually high measured U/Pb (Fig. 3*a*). It is possible to achieve the largest offsets in Pb isotopic composition at Madeira with U/Pb as high as measured in the lavas in ~130 Myr, the age of the lithosphere (Fig. 2*c*). It is difficult, however, to explain these offsets with much lower U/Pb in the source and longer times, as this enhances the $^{207}Pb/^{204}Pb$ as well as the $^{206}Pb/^{204}Pb$ ratios. A similar case was previously made for the source regions of the Cameroon line c.o.b.[7]. We therefore interpret the isotope

data for these two regions as indicating that the high U/Pb ratios of the lavas are also features of the source, with the age of U/Pb fractionation being comparable to the age of the lithosphere. The similarity between modelled and measured U/Pb ratios indicates that there was only minor fractionation of U/Pb during the partial melting that produced the lavas, consistent with the very low mineral-melt partition coefficients that have been measured for U and Pb (refs 25, 26). The Trinidade data display less pronounced offsets despite having high U/Pb, consistent with the younger age of the lithosphere at this location (Fig. 1). But the measured U/Pb ratios are variable and not correlated with $^{206}Pb/^{204}Pb$, implying some additional recent U/Pb fractionation, presumably associated with magma generation and differentiation. The Pb isotope data for other islands located in areas of old lithosphere, Fernando de Noronha, Cape Verdes and the oceanic Cameroon line (Fig. 1), tend to be only slightly high in $^{206}Pb/^{204}Pb$ for a given $^{207}Pb/^{204}Pb$ (Fig. 2*c*), as expected given the lower average U/Pb ratios of lavas from these islands (Fig. 3*a*).

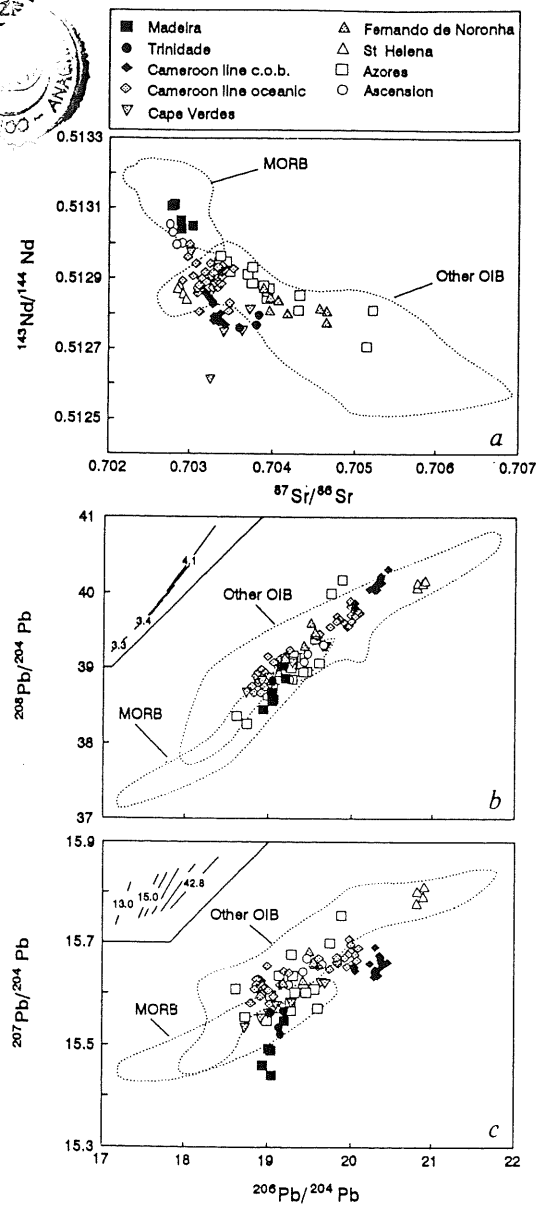

FIG. 2 Plots of *a*, Sr and Nd, and *b*, *c*, Pb isotopic compositions of lavas from the central Atlantic islands plus data for other OIB and MORB from the literature (Table 1 and refs. 7, 12–19). Where possible, we have plotted only samples for which U, Pb, Nd, and Sm data from isotope dilution, and major- and trace-element data from X-ray fluorescence were available. Comparisons with published data for central Atlantic islands are restricted to samples of common rock types, mainly transitional basalts, alkali basalts and basanites with a few nephelinites. Inserts to *b* and *c* show the changes expected in the Pb isotopic composition of a model array of data over a period of 130 Myr with μ ($^{238}U/^{204}Pb$) values comparable to those found in the erupted basalts. The array to the far left mimics the lead isotopic compositions at 130 Myr. The series of arrays to the right are present-day arrays produced by variable increases in μ and κ ($^{232}Th/^{238}U$) at 130 Myr. It is assumed that the μ and κ ratios in the precursor source, that is before enrichment, were variable in proportion to their respective Pb isotope ratios. The μ and κ produced in the source during enrichment at 130 Myr vary in proportion to the precursor source ratios, so the resultant Pb isotope arrays have different slopes. The average μ and κ are shown for each of the two most extreme arrays.

The respective portions of precursor mantle for Madeira and the Cameroon line c.o.b. before their enrichment in trace elements were radically different from each other. The Cameroon line basaltic magmas have OIB-like isotopic compositions and are thought to be derived by melting of a fossil plume, the head of which became fractionated in U/Pb about 125 Myr ago[7,14]. In contrast, the Madeira basalts have $^{87}Sr/^{86}Sr$, $^{143}Nd/^{144}Nd$ and $^{207}Pb/^{204}Pb$ ratios that are similar to modern MORB (Fig. 2*a*), and among the most extreme yet measured for OIB. Therefore, the most likely origin for the Madeira basalts is in upper-mantle MORB source material that was enriched $\sim 10^8$ yr ago. Clearly the trace-element enrichment process responsible for the offsets in Pb isotopic composition in Fig. 2*c* is largely independent of the exact precursor material and the longer-term heterogeneity of the mantle[1-6].

The incompatible element ratio K/U is considered uniform in MORB, a feature that is thought to reflect similar bulk partition coefficients for K and U such that there is negligible fractionation during melting[28]. In contrast, U is generally considered significantly more incompatible than Pb during melting[7,16,26,27]. Therefore, if the degree of melting is such that U/Pb ratios of OIB reflect their source compositions, the K/U ratios must also do so, unless there are phases in the OIB source that selectively fractionate K from U. A similar argument can be made for Ce/Pb ratios[29]. Lavas from Ascension and the Azores, close to the Mid-Atlantic Ridge, have K/U ratios that are similar to average MORB (Fig. 3*b*), whereas St Helena and centres from areas of old oceanic lithosphere have considerably lower ratios. The centres in oldest lithosphere (>100 Myr) with higher average U/Pb also have lower average K/U, suggesting that the process that fractionates the former may also be responsible for fractionation of the latter. Overall the average K/U and U/Pb ratios define a broad hyperbolic trend that may reflect mixing, but is more likely to indicate a process that fractionates both K and Pb relative to U (Fig. 3*b*). The centres with high U/Pb also have higher average Ce/Pb than most basalts[29] (Fig. 3*c*) If the U/Pb ratios are representative of their sources and were fractionated at the time of formation of the oceanic lithosphere, this must also be true of the Ce/Pb ratios.

The average Nd isotopic compositions of central Atlantic OIB correlate with their respective average Sm/Nd (Fig. 3*d*), although the average Madeira composition lies away from the trend defined by the other islands. Unlike combined Pb isotope data, Nd isotopic compositions cannot uniquely define both parent/daughter ratios and time. Assuming that average measured Sm/Nd ratios are lower than those of their source regions, the trend for most of the islands suggests that the age of the Nd isotopic heterogeneity is less than ~1 Gyr. To generate the range in Nd isotopic composition over the 130 Myr modelled for the Pb isotope data, however, requires excessively large variation in source Sm/Nd and does not explain the collinearity for islands with different lithospheric age. Therefore the Nd isotope data reflect long-term heterogeneity, and provide evidence that the process that fractionated U/Pb resulted in little fractionation of Sm/Nd. Similarly the melting that produced most of the erupted lavas resulted in a limited and/or systematic fractionation of Sm/Nd. This may be the result of

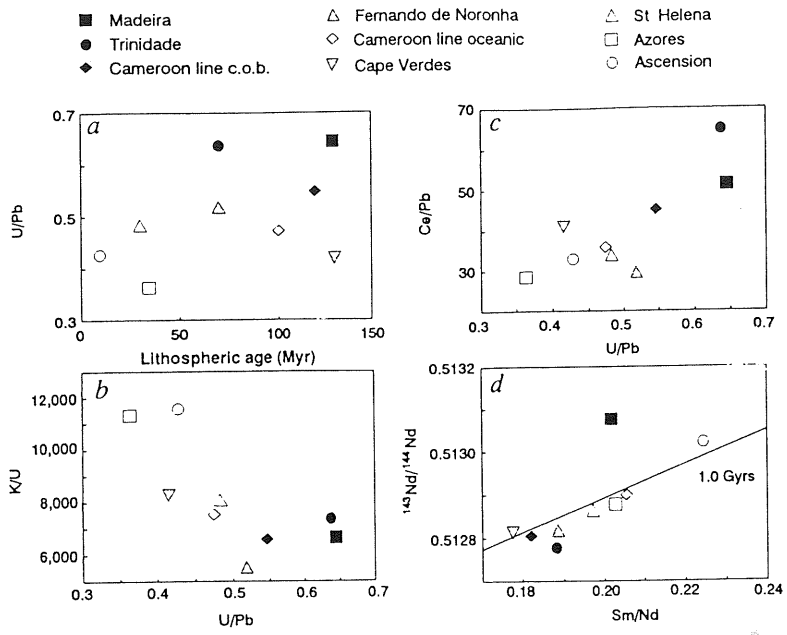

FIG. 3 Average U/Pb for each central Atlantic island as a function of lithospheric age; *b*, average K/U ratio against U/Pb ratio; *c*, average Ce/Pb ratio against U/Pb ratio and *d*, Nd isotope composition against Sm/Nd ratio. Data are from refs 7, 12-16, 20, 24 from Table 1 and our unpublished work.

low-pressure melting. The deviation of the average Madeira composition from the correlation for the other islands supports the view that the origins of the Madeira magmas are distinct in being derived by small degrees of partial melting at high pressure in the garnet stability field, as garnet would cause fractionation of the rare earth elements[23].

Several processes may be considered potentially responsible for the fractionations in U/Pb, Ce/Pb and K/U at the time of lithospheric growth. The melt regimes under ridges and hotspots are usually modelled as regions that are zoned laterally and vertically with respect to degree of partial melting[4,27,30-32]. Plume heads may be re-enriched by percolation of small-degree partial melts, such as nephelinitic magmas[7,30]. But there is little evidence that the U/Pb ratios of the source regions of the lavas studied here were fractionated simply by enriched small-degree partial melts. The inverse correlation of measured Sm/Nd and U/Pb for individual samples in the Cameroon line[7], and Trinidade (Table 1), implies that the fractionation of these trace element ratios is linked, but the average measured U/Pb and Sm/Nd ratios shown in Fig. 3 are not correlated, although both are source-related. Furthermore, small-degree partial melting in the presence of only the main upper-mantle mineral phases (assuming plagioclase is not involved) should not produce a positive correlation between U/Pb and Ce/Pb (Fig. 3*c*) on the basis of published mineral-melt distribution coefficients[25-27]. Minor buffering phases such as phlogopite and carbonates, which may play a role in low-degree partial melting of the mantle[6,30], have been invoked as an explanation for high U/Pb in areas of old continental lithosphere[10], but there is no obvious phase that will buffer K and Pb to produce the effect observed in Fig. 3*b*, without also affecting Ba or Ti; Ba/Ce ratios of central Atlantic OIB are in fact relatively uniform. Low-viscosity carbonatitic liquids may separate from immiscible nephelinitic liquids at small degrees of melting with concomitant fractionation of incompatible elements. This might explain the extreme U/Pb and Sm/Nd fractionations found in Trinidade and Cameroon line nephelinites. Nevertheless, although carbonatitic liquids may transport incompatible elements efficiently through the mantle[32], calculated compositions using experimental partition coefficients[33] cannot reproduce the fractionations shown in Fig. 3. A more speculative explanation is that there is a low-density, low-viscosity, subsolidus fluid phase associated with nephelinite magma generation but at greater depth below the melt zone, analogous to that suggested for Hawaii[30] into which, in the absence of phlogopite, K and Pb may preferentially partition[34] relative to U and the light rare earth elements. This fluid phase may migrate and be consumed in melting reactions elsewhere, or rise as a low-viscosity fluid[35], causing metasomatism in refractory lithosphere away from the melt zone. The low concentrations of volatiles in MORB glasses[36] argue against this explanation.

Whatever the exact mechanism for U/Pb fractionation, it seems to occur at shallow depths in the mantle at about the time of formation of the local oceanic lithosphere. The mantle currently being sampled at a distal ocean island must have undergone fractionation of U/Pb when it was located close to a cooling ridge (in the case of Madeira) or a cooling plume head (in the case of the Cameroon line). The sources of the Cameroon line, Trinidade and Madeira magmas have clearly resided in the upper mantle since the oceanic lithosphere was formed, and have not been displaced laterally by asthenospheric flow relative to the lithosphere since that time[7]. These portions of the mantle may now be melted preferentially in relatively undiluted form, away from the present ridge, by rising plumes[37] or hot zones[14] because they are enriched in low-temperature melting fractions incorporated at the time of U/Pb fractionation, and because of a lower geothermal gradient in areas of old thick lithosphere where the peridotite solidus is at greater depth. Elsewhere, such components are diluted by the larger volumes of magma generated at ridges and by rising plumes capable of ascending to shallower depths where the lithosphere is thin. The trace-element fractionations cannot, however, be explained simply as the product of small degrees of partial melting in areas of thicker lithosphere. Rather, storage of fractionated components for tens of millions of years is required. Such a model is endorsed by $^3He/^4He$ ratios lower than in MORB for the Cameroon line[38], suggesting a history of U enrichment. Finally, it should be noted that high U/Pb does not survive for long in the convecting mantle; otherwise the magnitude of Pb isotopic heterogeneity in basalts[1-6] would be greatly increased. □

Received 30 March; accepted 20 August 1992.

1. Hofmann, A. W. & White, W. M. *Earth planet. Sci. Lett.* **57**, 421-436 (1982).
2. McKenzie, D. & O'Nions, R. K. *Nature* **301**, 229-231 (1983).
3. Allègre, C. J., Hamelin, B., Provost, A. & Dupré, B. *Earth planet. Sci. Lett.* **81**, 319-337 (1986).
4. Galer, S. J. G. & O'Nions, R. K. *Chem. Geol.* **56**, 45-61 (1986).
5. Zindler, A. & Hart, S. *A. Rev. Earth planet. Sci.* **14**, 493-571 (1986).
6. Galer, S. J. G. & O'Nions, R. K. *Nature* **316**, 776-782 (1985).
7. Halliday, A. N. *et al. Nature* **347**, 523-528 (1990).
8. Emery, K. O & Uchupi, E. *The Geology of the Atlantic Ocean* (Springer, New York, 1984).

9. Vollmer, R. & Norry, M. J. *Nature* **301**, 141-143 (1983).
10. Hawkesworth, C. J., Kempton, P. D., Rogers, N. W., Ellam, R. M. & van Calsteren, P. W. *Earth planet. Sci. Lett.* **96**, 256-268 (1990).
11. Hart, S. R. *Nature* **309**, 753-757 (1984).
12. Sun, S.-S. & McDonough, W. F. in *Magmatism in the Ocean Basins* (ed. Saunders, A. D. & Norry, M. J.) 313-345 (Geol. Soc. Spec. Publ. No. 42, Blackwell Scientific, Oxford, 1989).
13. Davies, G. R., Norry, M. J., Gerlach, D. C. & Cliff, R. A. in *Magmatism in the Ocean Basins* (ed. Saunders, A. D. & Norry, M. J.) 231-255 (Geol. Soc. Spec. Publ. No. 42, Blackwell Scientific, Oxford, 1989).
14. Halliday, A. N., Dickin, A. P., Fallick, A. E. & Fitton, J. G. *J. Petrol.* **29**, 181-211 (1988).
15. Gerlach, D. C., Cliff, R. A., Davies, G. R., Norry, M. & Hodgson, N. *Geochim. cosmochim. Acta* **52**, 2979-2992 (1988).
16. Newsom, H. E., White, W. M., Jochum, K. P. & Hofmann, A. W. *Earth planet. Sci. Lett.* **80**, 299-313 (1986).
17. Ito, E., White, W. M. & Gopel, C. *Chem. Geol.* **62**, 157-176 (1987).
18. Palacz, Z. A. & Saunders, A. D. *Earth planet. Sci. Lett.* **79**, 270-280 (1986).
19. White, W. M. & Hofmann, A. W. *Nature* **196**, 821-825 (1982).
20. Gerlach, D. C., Stormer, J. C. Jr & Mueller, P. A. *Earth planet. Sci. Lett.* **85**, 129-144 (1987).
21. Mitchell-Thomé, R. G. *Geology of the South Atlantic Islands* (Gebrüder Borntraeger, Berlin, 1970).
22. Mitchell-Thomé, R. G. *Geology of the Middle Atlantic Islands* (Gebrüder Borntraeger, Berlin 1976).
23. Hughes, D. J. & Brown, G. C. *Contrib. Mineral. Petrol.* **37**, 91-109 (1972).
24. Fitton, J. G. & Dunlop, H. M. *Earth planet. Sci. Lett.* **72**, 23-38 (1985).
25. Seitz, M. G. *Yb Carnegie Instn Wash.* **72**, 551-553 (1973).
26. Watson, E. B., Ben Othman, D., Luck, J.-M. & Hoffmann, A. W. *Chem. Geol.* **62**, 191-208 (1987).
27. McKenzie, D. & O'Nions, R. K. *J. Petrol.* **32**, 1021-1091 (1991).
28. Jochum, K. P., Hofmann, A. W., Ito, E., Seufert, H. M. & White, W. M. *Nature* **306**, 431-436 (1984).
29. Hofmann, A. W., Jochum, K. P., Seufert, M. & White, W. M. *Earth planet Sci. Lett.* **79**, 33-45 (1986).
30. Wyllie, P. J. *J. geophys. Res.* **93**, 4171-4181 (1988).
31. McKenzie, D. *Earth planet. Sci. Lett.* **74**, 81-91 (1985).
32. McKenzie, D. *Earth planet. Sci. Lett.* **72**, 149-157 (1985).
33. Fielding, K. D., Fitton, J. G., Ford, C. E. & Hinton, R. W. *Terra Abstr.* **3**, 419 (1991).
34. Schneider, M. E. & Eggler, D. H. *Geochim. Cosmochim. Acta* **50**, 711-724 (1986).
35. Watson, E. B., Brennan, J. M. & Baker, D. R. in *Continental Mantle* (ed. Menzies, M.) 111-124 (Clarendon, Oxford, 1990).
36. Michael, P. J. *Geochim. cosmochim. Acta* **52**, 555-566 (1988).
37. Richards, M. A. & Griffiths, R. W. *Nature* **342**, 900-902 (1989).
38. Sano, Y., Wakita, H., Ohsumi, T. & Kusakabe, M. *Geophys. Res. Lett.* **14**, 1039-1041 (1987).

ACKNOWLEDGEMENTS. We thank K. O'Nions, R. Lange and Y. Zhang for discussions, colleagues in the Radiogenic Isotope Geochemistry Laboratory for criticism of the text, and W. White for a review. The research was supported by NSF grants to A.N.H.

A sharp and flat section of the core–mantle boundary

John E. Vidale & Harley M. Benz

United States Geological Survey, Branch of Seismology,
345 Middlefield Road MS 977, Menlo Park, California 94025, USA

THE transition zone between the Earth's core and mantle plays an important role as a boundary layer for mantle and core convection[1]. This zone conducts a large amount of heat from the core to the mantle, and contains at least one thermal boundary layer[2,3]; the proximity of reactive silicates and molten iron leads to the possibility of zones of intermediate composition[4]. Here we investigate one region of the core–mantle boundary using seismic waves that are converted from shear to compressional waves by reflection at the boundary. The use of this phase (known as ScP), the large number of receiving stations, and the large aperture of our array all provide higher resolution than has previously been possible[5–7]. For the 350-km-long section of the core–mantle boundary under the northeast Pacific sampled by the reflections, the local boundary topography has an amplitude of less than 500 m, no sharp radial gradients exist in the 400 km above the boundary, and the mantle-to-core transition occurs over less than 1 km. The simplicity of the structure near and above the core–mantle boundary argues against chemical heterogeneity at the base of the mantle in this location.

The regional seismic networks of the United States and Canada routinely record local and distant earthquakes, mainly in order to monitor active faults within the networks. Together, these networks include more than 1,500 stations and span a wide aperture. This set of receivers is ideal for observing short-period seismic waves from distant earthquakes across larger distances than previously possible[8].

The phase ScP travels from the earthquake to the core-mantle boundary (CMB) as an S wave, then converts to a P wave for the remaining path to the receiver (Fig. 1*a*). ScP appears in a particularly quiet interval on seismograms for an earthquake that occurred on 13 March 1992, 180 km beneath the Andreanof Islands (magnitude m_b 6.1, 52.8° N, 178.8° W). We analyse seismograms from the University of Washington Seismic Network (125 stations), the Southern California Seismic Network (216 stations) and the Northern California Seismic Network (405 stations). The high signal-to-noise ratios of these seismograms will reveal the degree of lateral variation in structure near the CMB, the presence or absence of structure above the CMB and the sharpness of the CMB. These data are only sensitive to lateral variations in the CMB with wavelengths of 50 to 200 km, these limits arising from the limitations in resolution of 1-Hz seismic waves and the 15° aperture of the array, respectively. The data are sensitive to radial variations with wavelengths up to 10 km, beyond which insufficient short-period energy is reflected.

A smaller (m_b 5.3) event on 27 March 1992 (52.8° N, 174.0° W, 190 km depth) produced a particularly sharp set of arrivals, but was only available on the Northern California Seismic Network. The simplicity of the earthquake allows a direct measure of the simplicity of the CMB.

ScP is prominent in the distance range from 30° to 70° because the conversion coefficient at the CMB is large. The main source of short-period noise in this time interval is the coda of the P wave, which attenuates rapidly with time after the P wave passes. We study the CMB with the ScP phase rather than the more traditional choice of PcP[5–7] (Fig. 1) because ScP arrives 4 minutes later with a more favourable signal-to-noise ratio.

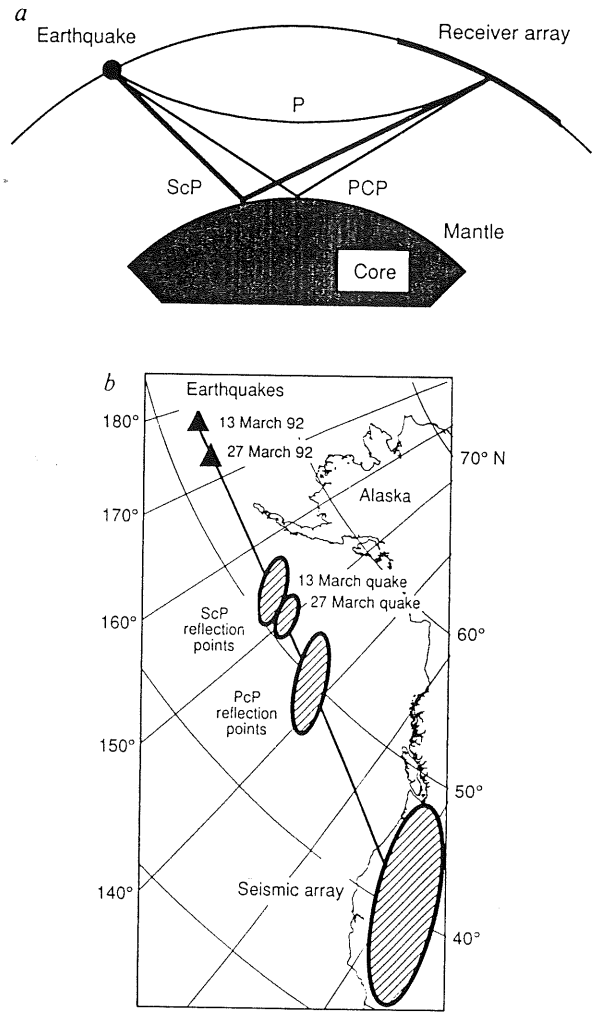

FIG. 1 Schematic ray paths (*a*) and bounce points at the core-mantle boundary (*b*) for the seismic waves analysed here.